HHS Public Access

Author manuscript

ACS Sens. Author manuscript; available in PMC 2020 August 23.

Published in final edited form as:

ACS Sens. 2019 August 23; 4(8): 2205–2212. doi:10.1021/acssensors.9b01201.

Optical tracking of nanometer-scale cellular membrane deformation associated with single vesicle release

Fenni Zhang[*,1,3], **Yan Guan**[*,1,3], **Yunze Yang**[1,3], **Ashley Hunt**[1], **Shaopeng Wang**[1], **Hong-Yuan Chen**[2], **Nongjian Tao**[**,1,3]

[1]Biodesign Center for Bioelectronics and Biosensors, Arizona State University, Tempe, AZ 85287, USA.

[2]State Key Laboratory of Analytical Chemistry for Life Science, School of Chemistry and Chemical Engineering, Nanjing University, Nanjing 210093, China

[3]School of Electrical Computer and Energy Engineering, Arizona State University, Tempe, Arizona 85287, USA.

Abstract

Exocytosis involves interactions between secretory vesicles and plasma membrane. Studying the membrane response is thus critical to the understanding of this important cellular process and to differentiate different mediator release patterns. Here we introduce a label-free optical imaging method to detect the vesicle-membrane interaction induced membrane deformation associated with single exocytosis in mast cells. We show that the plasma membrane expands by a few tens of nm accompanying each vesicle release event, but the dynamics of the membrane deformation varies from cell to cell, which reflect different exocytosis processes. Combining the temporal and spatial information allows us to resolve complex vesicle release processes, such as two vesicle release events that occur closely in time and location. Simultaneous following of a vesicle release with fluorescence and membrane deformation tracking further allows us to determine the propagation speed of the vesicle-release induced membrane deformation along the cell surface, which has an average value of 5.2 ± 1.8 μm/s.

Graphical Abstract

**Corresponding author: njtao@asu.edu.
*These authors contribute equally to the project.

ASSOCIATED CONTENT

Supporting Information.

Supporting Information Available: Calibration differential optical tracking of cell membrane deformation; Optical synchronization; Cell membrane deformation at different locations; Membrane deformation histogram of individual granule release events in different cells; Examples of different patterns of granule release-induced membrane deformation;

The authors declare no competing financial interest.

Data availability

The datasets generated during and/or analyzed during the current study are available from the corresponding author on reasonable request.

Code availability

Computer codes used for cell membrane deformation tracking that support the findings of this study are available from the corresponding author on request.

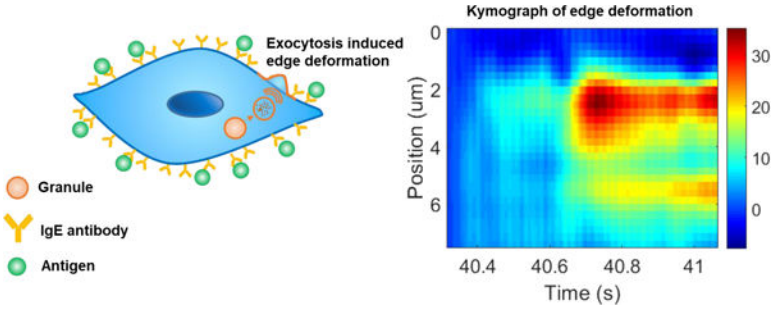

Keywords

exocytosis; membrane deformation; mast cell; label-free; phase contrast imaging

Exocytosis is a basic cellular process that involves membrane fusion and vesicular secretion of intracellular substances, such as neurotransmitters, exosomes, hormones and enzymes, which are critical for various cellular functions, including cell-cell communications, immune responses, synaptic signal transmission and cellular metabolism.[1–3] Uncontrolled exocytosis results in cell proliferation, migration, invasion and tumor development.[4] To monitor the rapid exocytosis process, the detection methods require high sensitivity and high temporal resolution. The current available techniques include electrophysiological recording, electrochemical detection, microscopic imaging and spectroscopic analysis.[5–9] The electrophysiology method measures cellular membrane capacitance by the whole cell patch clamp technique.[10–13] Although powerful, the membrane capacitance reflects an overall cellular surface area change, which does not provide the spatial information of an exocytosis event. The electrophysiological recording method, on the other hand, has limited throughput because it measures one cell at a time. The electrochemical method detects the oxidation current of molecules released from vesicles with microelectrodes,[14–20] which can quantify the amount of the secretory molecules and monitor the dynamic process of fusion with high sensitivity[21–22]. But it is limited to vesicles containing electroactive species. The fluorescence microscopy imaging approach can detect individual exocytosis events with high spatial resolution, [23–28] in which the total internal reflection fluorescence microscopy (TIRFM) is commonly used to visualize the vesicle movement and fusion[29–30]. However, the temporal resolution of fluorescence imaging is limited by the number of photons emitted from the fluorophores[31]. Also, the fluorescence imaging signal does not provide direct information on the cell membrane mechanical deformation.

Here we report a label-free method to image single vesicle fusion-induced cellular plasma membrane deformation with ~10 nm precision and milliseconds temporal resolution in mast cells. Mast cells have been established as the key effector cells in allergic disorder, more importantly, they are associated with diverse immunological regulations[32–34]. During the vesicle exocytosis process, different mediators/exosomes are released for various functions[32], which can be used for disease diagnosis and prognosis[35]. However, the mechanisms underlying differential mediator release are poorly known[36]. By monitoring the cellular membrane response during single vesicle release, we are able to differentiate different secretory processes, which is critical for cell phenotyping and for disease diagnosis

and treatment. Various optical techniques have been developed for detecting cell membrane fluctuations, including phase, scattering and interference based methods[37–42]. This work combines the phase contrast imaging with a differential optical tracking algorithm to track displacement at cell edges. Comparing to fluorescence imaging, the phase contrast imaging is label-free and provides high-contrast images with decent temporal resolution, which can reveal detailed kinetics of the rapid exocytosis process. We monitored the vesicle release events in single cells and map the spatial distribution of the cell membrane deformation induced by vesicle fusion and its evolution over time. From the temporal and spatial patterns, we identified different membrane responses, corresponding to different exocytosis modes, such as full fusion and "kiss-and-run" exocytosis. Simultaneous recording of cell membrane deformation and fluorescence further allowed us to validate the single exocytosis and study the propagation of exocytosis-induced membrane deformation along cellular membrane surface. This work provides new insights into exocytosis, and the nm-membrane deformation tracking capability may be extended to study other cellular processes, such as endocytosis for drug delivery, and discriminate cell phenotypes with different mediator release for disease diagnosis.

Methods and Methods

Materials

2,4-dinitrophenylated albumin from bovine serum (DNP-BSA) was purchased from Life Technologies (Carlsbad, CA). Monoclonal anti-Dinitrophenyl (anti-DNP) IgE, fluorescein isothiocyanate-dextran (FITC-dextran) and serotonin molecules were purchased from Sigma-Aldrich (St. Louis, MO). All solutions used in the experiments were prepared with home-made fresh extracellular buffer (135 mM NaCl, 5 mM KCl, 20 mM HEPES, 1.8 mM $CaCl_2$, 1 mM $MgCl_2$, 5.6 mM glucose, pH = 7.4). All reagents were analytical grade from Sigma-Aldrich, except those stated.

Cell culture

RBL-2H3 cells were purchased from American Type Culture Collection (ATCC, Rockville, MD). RBL-2H3 cells were cultured in a humidity incubator at 37°C with 5% CO_2 and 70% relative humidity. Eagle's Minimum Essential Medium (EMEM, ATCC 30–2003) with 15% heat inactivated Fetal Bovine Serum (FBS, Life Technologies, Carlsbad, CA) and 1% penicillin-streptomycin (BioWhittaker, Basel, Switzerland) were used as culture medium for cell growth. RBL-2H3 cells were cultured in 25 cm^2 flask and passaged when approximately 80% confluence was reached. 0.05% trypsin-EDTA (Life Technologies, Carlsbad, CA) was used for cell passage.

Vesicle release initiation

RBL-2H3 cells were transferred to 35 mm diameter tissue culture petri dish (Corning Inc., Corning, NY) for overnight culture. 200 μM serotonin, 0.5 μg/ml monoclonal anti-Dinitrophenyl (anti-DNP) IgE and 1 mg/ml fluorescein isothiocyanate-dextran (FITC-dextran, molecular weight 150 KDa) were added to the culture medium for vesicle release preparation. Serotonin was used to increase the size of vesicle, and this concentration has no obvious effects on exocytosis kinetics [43–44]. FITC-dextran was used to label the cells for

simultaneous tracking of vesicle release with fluorescence imaging and cell membrane deformation. Anti-DNP IgE was used to bind with the cell surface expressed high affinity IgE receptors (FcεRI). Antigen, 2,4-dinitrophenylated albumin from bovine serum (DNP-BSA), was introduced to bind to anti-DNP IgE and cross-link FcεRI, which initiated a signaling cascade leading to vesicle exocytosis of the cells and release of chemical mediators[44].

Before each measurement, the cells were rinsed with 0.1% BSA in an extracellular buffer (135 mM NaCl, 5 mM KCl, 20 mM HEPES, 1.8 mM $CaCl_2$, 1 mM $MgCl_2$, 5.6 mM glucose, pH=7.4) for three times to block the surface followed by another three times wash with extracellular buffer only to remove extra BSA. A petri dish with cells in 1 mL extracellular buffer was transferred to the microscope, and phase contrast and fluorescent images were recorded after addition of 1 mL of 5 μg/ml DNP-BSA into the petri dish.

Optical setup

An inverted microscope (Olympus IX81) equipped with a phase 2 condenser and phase 2 40X objective was used with illumination from the top of the sample cells (Fig. 1A). The phase contrast image was recorded by a Hamamatsu camera with frame rates up to 400 fps for tracking membrane deformation. A set of optical filters (Ex420–480/Em515) was used for fluorescence excitation and collection, and the fluorescent image was recorded at a frame rate of 8 fps with a second Hamamatsu camera for vesicle exocytosis validation. To synchronize the recording time of the phase contrast and the fluorescent image sequences, a shutter was used to cut off the common light path of fluorescent and phase contrast imaging and aligning the two image sequences allow synchronization (Fig. S2).

Fluorescent imaging

Fluorescent imaging is used for single exocytosis validation. The fluorescence emission was from the excitation of fluorescein isothiocyanate–dextran (FITC-dextran), which was added to the cell before overnight culture. FITC-dextran was sensitive to the pH of the medium. Before vesicle release, the fluorescence signal of FITC-dextran was quenched by the low-pH of vesicle medium, and during vesicle release, the fluorescence signal was activated by neutral pH extracellular medium. The fluorescence image was captured simultaneously with the phase contrast images for vesicle release validation.

Signal analysis

The membrane deformation measured with the differential edge tracking method was represented in color scale (Supporting Information S-1). The spatial distribution of the membrane deformation along a cell edge was tracked by extracting the membrane deformation magnitudes of different positions near the time point where the deformation is maximum, and the temporal profile of the membrane deformation at different locations along the cell edge was extracted. By averaging the membrane deformations at different locations, an average temporal profile of the vesicle release was obtained. By fitting the spatial distribution with Gaussians, the center of the vesicle release and the full width at half maximum (FWHM) of the spatial distribution were obtained, and the fitted peaks indicated the number of the exocytosis events.

Results and discussion

Detection principle

We studied vesicle release in RBL-2H3, a rat basophilic leukemia cell line (Fig. 1). The RBL-2H3 cell surface was expressed with immunoglobulin E (IgE) receptors (FcεRI),[24] which were activated by IgE antibody binding. Exocytosis in the cells was initiated by specific binding of an antigen to the antibody,[25] during which the vesicle docks and interacts with the plasma membrane of the cells (Fig. 1D). To investigate the membrane responses during vesicle release, we used a dual-optical system to simultaneously record phase contrast and fluorescence images of the cells (Fig. 1A). The phase contrast imaging, together with a differential optical tracking algorithm described below, allows tracking of nm-scale membrane deformation associated with vesicle release, and the fluorescence imaging based on the pH sensitive fluorescent dye helped validate individual vesicle release events tracked by the membrane deformation. Figs. 1B and 1C show a typical phase contrast image and the fluorescence image of a cell, respectively, where the red arrows mark the locations of vesicle release.

Because of the small sizes of the vesicles, the vesicle release-induced cell membrane deformation is expected to be small. To measure the small deformation, we used a differential optical tracking method to measure position changes in the cell edge associated with the membrane deformation. The differential optical method includes the following steps. First, the edge of a cell is identified from the phase contrast image (Fig. 1B). Second, a rectangular region of interest (ROI) is selected such that the edge of a cell passes through the center of the ROI. The rectangular ROI is then divided into two equal halves, one half is inside of the cell (red) and the other half falls outside of the cell (blue, Fig. 1D). When the cell membrane deforms, the image intensity of one half (I_1) increases while the other half (I_2) decreases. Third, the differential image intensity of the two halves is defined as $(I_1-I_2)/(I_1+I_2)$, which is used to determine the cell membrane deformation at each ROI location (Supporting Information S1). To convert the differential image intensity to an actual cell edge membrane deformation, calibration was performed using a procedure described in Supporting Information Fig. S1. This differential optical detection subtracts the common noise in optical system, thus providing excellent detection limit.

Vesicle release measured by tracking cell edge deformation

We studied exocytosis in different cells and observed membrane responses with variable temporal and spatial characteristics. One reprehensive response is a rapid expansion of the cell membrane upon vesicle release followed by slow or little recovery. One such example is shown in Fig. 2A (top), which plots the membrane deformation of a cell associated with a vesicle release event, revealing a rapid membrane deformation by ~56 nm over 0.275 s followed by slow recovery, where I, II, III and IV mark different time points during the process. The corresponding snapshots of the phase contrast images at these time points are labeled by I, II, III and IV in Fig. 2A (bottom). The cell deformation is too small to be directly visible in the phase contrast images, so the magnitude of the cell deformation determined by the differential tracking method is represented with a color scale overlaid on

the phase contrast images. The insets in Figs. 2A (bottom) are zoom-in images of the cell deformation.

To validate that this stepwise cell expansion is due to a vesicle release event, we compared the cell deformation data (Fig. 2A) with the simultaneously recorded fluorescence images (Fig. 2B). The fluorescence images (after background subtraction) show a bright spot due to fluorescence emission at the location marked by a dashed circle (Figs. 2B, bottom). The location of the observed fluorescence emission coincides with that of cell expansion, which confirms that the cell edge expansion is due to vesicle release. In contrast to the cell deformation in Fig. 2A (top), the fluorescent emission in Fig. 2B (top) shows a rapid increase followed by a rapid decrease during the vesicle release event, corresponding to membrane fusion (I), during fusion (II) and diffusion of fluorescein isothiocyanate–dextran (FITC-dextran)(III and IV). To further confirm that the observed membrane expansion was related to vesicle release, we examined membrane deformation at other locations along the cell edge and detected cell deformation only near the location of the fluorescence emission (Supporting Information Fig. S3).

Fig. 3A shows another membrane response during vesicle release. Unlike the stepwise expansion shown in Fig. 2A, this is pulse-like, i.e., a rapid expansion followed by immediate recovery. Fig. 3A (top) is the temporal profile of this deformation, where I, II, III and IV mark different stages of this vesicle exocytosis event. The time duration is 0.020 s, much faster than the stepwise expansion in Fig. 2A. The location of the cell deformation is marked by a red arrow in the snapshots of the phase contrast images at the time points of I, II, III and IV (Fig. 3A, bottom). The simultaneously recorded fluorescence images during this vesicle release event shows an obvious bright spot near the cell deformation position (Fig. 3B, bottom). The temporal profile of the fluorescence emission displays a sharp increase followed by a decrease, which shows smaller intensity and shorter duration compared with that in stepwise membrane expansion (Fig. 3B, top). We also tracked cell deformation along the entire cell edge and detected significant cell deformation only near the fluorescence emission spot.

We analyzed 130 individual vesicle release events from the fluorescent signals in 52 cells and found that 110 vesicle release events showed detectable edge deformation. The histogram distribution of the vesicle release induced membrane deformation is presented in Fig. S4. For the cells that show deformation during vesicle release, ~90% of them display stepwise deformation and ~10% show pulse-like deformation. The stepwise cell deformation indicates an increase in the cell area that sustains after vesicle release, which is consistent with the stepwise capacitance increases observed for full fusion exocytosis.[45] In a full fusion process, a vesicle fuses into the cell membrane after releasing its chemical content, which leads to an increase in the cell surface area, and thus membrane expansion. In contrast, the pulse-like cell deformation is transient, similar to the capacitance spikes observed with patch-clamp techniques in ‘kiss and run’ exocytosis.[45] In ‘kiss-and-run’ process, the vesicle interacts with the cell membrane and releases its chemical content via a transient fusion pore, leading to a transient expansion of the cell membrane. The fluorescent signal of the pulse-like expansion is smaller than that of the stepwise expansion, which is likely due to the partial release of vesicle in ‘kiss-and-run’ process.[46–47]

Localized cell membrane deformation due to vesicle release.

The cell edge tracking method provides spatial and temporal resolutions, which helps resolve multiple vesicle releases that take place closely in time and location. Fig. 4A shows a cell that exhibits stepwise cell membrane deformation during vesicle exocytosis, where the color scale represents cell deformation magnitude. Fig. 4B plots the spatial distribution of the cell deformation near the time point where the deformation is maximum. Fitting the spatial distribution with a Gaussian function leads to a full width at half maximum (FWHM) of ~1.6 μm, which is the spread of the cell deformation near the location of vesicle release and the fitted single peak implies single vesicle release event. The temporal-spatial pattern, termed as Kymograph, along the cell edge of this vesicle release provides more complete information on the spatial distribution and temporal evolution of the cell deformation (Fig. 4C). Figs. 4D–F show a pulse-like cell deformation. In contrast to the example shown in Figs. 4A–C, the cell deformation in this case is more localized and decay rapidly over time. The corresponding Kymograph (Fig. 4F) of this vesicle release shows a well-defined spot, indicating that the membrane deformation is confined in both time and location.

Figs. 4G–I show a complex situation, where two vesicle release events occur closely in both time and location. The color representation of the cell deformation (Fig. 4G) reveals two bright (red) spots, each corresponding to a vesicle release event. The two vesicle release events are also shown as two peaks in the Gaussian fitting of the spatial distribution of the membrane deformation along the cell edge (Fig. 4H). The two-vesicle release events decay over time slowly without propagation along the cell edge as shown in the Kymograph (Fig. 4I). The Kymograph further reveals that one vesicle release event (marked by a black arrow) occurs ~0.1 s earlier than the second one (marked by a white arrow). Other examples of complex vesicle releases are given in Fig. S5. These complex vesicle releases are resolved because of the spatial and temporal resolutions of the present method.

The observed cell deformation during vesicle release is consistent with the capacitance measurement, which detects cell surface area increase[48]. Cell expansion is expected for a full fusion process of exocytosis[49–50], where a secretory vesicle docks onto the cell plasma membrane, forms a fusion pore and becomes fully incorporated with the cell membrane after releasing chemical contents in the vesicle to the extracellular medium. The incorporation of the vesicle into the cell membrane increase the area and detected as a stepwise expansion of cell edge. The pulse-like cell deformation is likely to be a ‘kiss-and-run’ process, which perturbs the cell membrane temporarily and observed as a transient cell deformation.

Propagation of vesicle release-induced membrane deformation.

Simultaneous recording of phase contrast and fluorescent images allowed us to determine vesicle exocytosis-induced cell membrane deformation propagation on a cell surface. Fig. 5 shows cell membrane deformation and fluorescence signals of four representative cells. The location of fluorescence emission in each case is in close proximity with the location of cell edge deformation (Figs. 5E–L), however, there is a time delay between the cell deformation and fluorescence emission. As shown in Figs. 5A to 5D, the fluorescence peaks are always ahead of the membrane expansion. This time delay indicates propagation of the membrane deformation from the location of vesicle release to the cell edge (Fig. 6B). From the

propagation distance and time delay, we determined the propagation speed of the membrane deformation along the cell surface in each cell (Fig. 6). There is a broad distribution in the propagation speed from cell to cell and the average speed is 5.2 ± 1.8 μm/s (n=24). This value is consistent with the membrane shape mediated wave propagation speed [51–52]. Mecahcnial waves have been detected in neurons, which is active and can be highly directional [53]. In contrast, the membrane deformation associated with vesicle release appears to be a passive response of the cell membrane and progagates in all directions.

Conclusions

By combining a high contrast phase imaging and differential optical tracking method, we show that the plasma membrane response near the cell edge to single vesicle exocytosis events can be tracked with nm precision and milliseconds temporal resolution. Using this capability, we have detected rapid membrane responses upon each vesicle release event in single cells. Despite large variability for different cells, two representative membrane deformations were found to be consistent with full fusion and ‘kiss-and-run’ exocytosis processes. The high spatial and temporal resolutions of the method allow to resolve complex vesicle release patterns, including multiple vesicles release events that occur closely in both time and position. Simultaneous tracking of each individual vesicle exocytosis events with both the fluorescence and cell deformation methods reveals propagation of the membrane deformation one cell surfaces with an average speed of 5 μm/s. This work presents a simple and label-free method to study single vesicle release events in single cells by tracking cell membrane deformation, which is not possible with the previous methods, and its high spatial and temporal resolutions offer new insights into the important processes of vesicle exocytosis in single cells and may be used to monitor the differential mediator release to different stimuli for cell characterization for disease study. Furthermore, this method can be extended to study other cellular processes, such as endocytosis for drug delivery.

Supplementary Material

Refer to Web version on PubMed Central for supplementary material.

Acknowledgements

Financial support from NIH (1R01GM124335) is acknowledged.

References

(1). Sudhof TC. The synaptic vesicle cycle. Annu Rev Neurosci 2004, 27, 509–547. [PubMed: 15217342]

(2). Katz B. The release of neural transmitter substances. Thomas: Springfield, Ill, 1969.

(3). Sudhof TC; Rizo J. Synaptic vesicle exocytosis. Cold Spring Harb Perspect Biol 2011, 3 (12), doi: 10.1101/cshperspect.a005637.

(4). Hendrix A; Westbroek W; Bracke M; De Wever O. An ex(o)citing machinery for invasive tumor growth. Cancer Res 2010, 70 (23), 9533–9537. [PubMed: 21098711]

(5). Angleson JK; Betz WJ. Monitoring secretion in real time: Capacitance, amperometry and fluorescence compared. Trends in neurosciences 1997, 20 (7), 281–287. [PubMed: 9223217]

(6). Tyler WJ; Murthy VN. Synaptic vesicles. Curr Biol 2004, 14 (8), R294–297. [PubMed: 15084295]

(7). Lemaitre F; Collignon MG; Amatore C. Recent advances in electrochemical detection of exocytosis. Electrochim Acta 2014, 140, 457–466.

(8). Fulop T; Radabaugh S; Smith C. Activity-dependent differential transmitter release in mouse adrenal chromaffin cells. J Neurosci 2005, 25 (32), 7324–7332. [PubMed: 16093382]

(9). Oleinick A; Svir I; Amatore C. 'Full fusion' is not ineluctable during vesicular exocytosis of neurotransmitters by endocrine cells. Proc Math Phys Eng Sci 2017, 473 (2197), 20160684. [PubMed: 28265193]

(10). Mellander L; Cans AS; Ewing AG. Electrochemical probes for detection and analysis of exocytosis and vesicles. Chemphyschem 2010, 11 (13), 2756–2763. [PubMed: 20737529]

(11). Neher E; Marty A. Discrete changes of cell membrane capacitance observed under conditions of enhanced secretion in bovine adrenal chromaffin cells. Proc Natl Acad Sci U S A 1982, 79 (21), 6712–6716. [PubMed: 6959149]

(12). Rituper B; Gucek A; Jorgacevski J; Flasker A; Kreft M; Zorec R. High-resolution membrane capacitance measurements for the study of exocytosis and endocytosis. Nat Protoc 2013, 8 (6), 1169–1183. [PubMed: 23702833]

(13). Thompson RE; Lindau M; Webb WW. Robust, high-resolution, whole cell patch-clamp capacitance measurements using square wave stimulation. Biophys J 2001, 81 (2), 937–948. [PubMed: 11463636]

(14). Wu W; Huang W; Wang W; Wang Z; Cheng J; Xu T; Zhang R; Chen Y; Liu J. Monitoring dopamine release from single living vesicles with nanoelectrodes. J Am Chem Soc 2005, 127 (25), 8914–8915. [PubMed: 15969544]

(15). Wang CT; Grishanin R; Earles CA; Chang PY; Martin TF; Chapman ER; Jackson MB. Synaptotagmin modulation of fusion pore kinetics in regulated exocytosis of dense-core vesicles. Science 2001, 294 (5544), 1111–1115. [PubMed: 11691996]

(16). Zhang B; Heien M; Santillo MF; Mellander L; Ewing AG. Temporal resolution in electrochemical imaging on single pc12 cells using amperometry and voltammetry at microelectrode arrays. Anal Chem 2011, 83 (2), 571–577. [PubMed: 21190375]

(17). Adams KL; Jena BK; Percival SJ; Zhang B. Highly sensitive detection of exocytotic dopamine release using a gold-nanoparticle-network microelectrode. Anal Chem 2011, 83 (3), 920–927. [PubMed: 21175175]

(18). Amatore C; Arbault S; Guille M; Lemaitre F. Electrochemical monitoring of single cell secretion: Vesicular exocytosis and oxidative stress. Chem Rev 2008, 108 (7), 2585–2621. [PubMed: 18620370]

(19). Zhang B; Adams KL; Luber SJ; Eves DJ; Heien ML; Ewing AG. Spatially and temporally resolved single-cell exocytosis utilizing individually addressable carbon microelectrode arrays. Anal Chem 2008, 80 (5), 1394–1400. [PubMed: 18232712]

(20). Li X; Dunevall J; Ewing AG. Quantitative chemical measurements of vesicular transmitters with electrochemical cytometry. Acc Chem Res 2016, 49 (10), 2347–2354. [PubMed: 27622924]

(21). Amatore C; Arbault S; Bonifas I; Guille M. Quantitative investigations of amperometric spike feet suggest different controlling factors of the fusion pore in exocytosis at chromaffin cells. Biophys Chem 2009, 143 (3), 124–131. [PubMed: 19501951]

(22). Amatore C; Arbault S; Bonifas I; Guille M; Lemaitre F; Verchier Y. Relationship between amperometric pre-spike feet and secretion granule composition in chromaffin cells: An overview. Biophys Chem 2007, 129 (2–3), 181–189. [PubMed: 17587484]

(23). Anantharam A; Onoa B; Edwards RH; Holz RW; Axelrod D. Localized topological changes of the plasma membrane upon exocytosis visualized by polarized tirfm. J Cell Biol 2010, 188 (3), 415–428. [PubMed: 20142424]

(24). Zenisek D; Steyer JA; Almers W. Transport, capture and exocytosis of single synaptic vesicles at active zones. Nature 2000, 406 (6798), 849–854. [PubMed: 10972279]

(25). Gaffield MA; Betz WJ. Imaging synaptic vesicle exocytosis and endocytosis with fm dyes. Nat Protoc 2006, 1 (6), 2916–2921. [PubMed: 17406552]

(26). Betz WJ; Mao F; Smith CB. Imaging exocytosis and endocytosis. Curr Opin Neurobiol 1996, 6 (3), 365–371. [PubMed: 8794083]

(27). Keighron JD; Ewing AG; Cans AS. Analytical tools to monitor exocytosis: A focus on new fluorescent probes and methods. Analyst 2012, 137 (8), 1755–1763. [PubMed: 22343677]

(28). Ge SC; Koseoglu S; Haynes CL. Bioanalytical tools for single-cell study of exocytosis. Anal. Bioanal. Chem 2010, 397 (8), 3281–3304. [PubMed: 20521141]

(29). Akopova I; Tatur S; Grygorczyk M; Luchowski R; Gryczynski I; Gryczynski Z; Borejdo J; Grygorczyk R. Imaging exocytosis of atp-containing vesicles with tirf microscopy in lung epithelial a549 cells. Purinerg Signal 2012, 8 (1), 59–70.

(30). Zhang Z; Wu Y; Wang Z; Dunning FM; Rehfuss J; Ramanan D; Chapman ER; Jackson MB. Release mode of large and small dense-core vesicles specified by different synaptotagmin isoforms in pc12 cells. Mol Biol Cell 2011, 22 (13), 2324–2336. [PubMed: 21551071]

(31). Huang B; Bates M; Zhuang X. Super-resolution fluorescence microscopy. Annu Rev Biochem 2009, 78, 993–1016. [PubMed: 19489737]

(32). Kormelink TG; Arkesteijn GJA; van de Lest CHA; Geerts WJC; Goerdayal SS; Altelaar MAF; Redegeld FA; Nolte-'t Hoen ENM; Wauben MHM. Mast cell degranulation is accompanied by the release of a selective subset of extracellular vesicles that contain mast cell-specific proteases. J Immunol 2016, 197 (8), 3382–3392. [PubMed: 27619994]

(33). Carroll-Portillo A; Surviladze Z; Cambi A; Lidke DS; Wilson BS. Mast cell synapses and exosomes: Membrane contacts for information exchange. Front Immunol 2012, 3, doi: 10.3389/fimmu.2012.00046.

(34). Xie GG; Yang HW; Peng X; Lin LH; Wang J; Lin K; Cui ZL; Li J; Xiao H; Liang YT; Li L. Mast cell exosomes can suppress allergic reactions by binding to ige. J Allergy Clin Immun 2018, 141 (2), 788–791. [PubMed: 28916187]

(35). Theoharides TC; Valent P; Akin C. Mast cells, mastocytosis, and related disorders. N Engl J Med 2015, 373 (19), 1885–1886.

(36). Moon TC; Befus AD; Kulka M. Mast cell mediators: Their differential release and the secretory pathways involved. Front Immunol 2014, 5, doi: 10.3389/fimmu.2014.00569.

(37). Brocca P; Cantu L; Corti M; Del Favero E; Motta S. Shape fluctuations of large unilamellar lipid vesicles observed by laser light scattering: Influence of the small-scale structure. Langmuir 2004, 20 (6), 2141–2148. [PubMed: 15835663]

(38). Popescu G; Ikeda T; Dasari RR; Feld MS. Diffraction phase microscopy for quantifying cell structure and dynamics. Opt Lett 2006, 31 (6), 775–777. [PubMed: 16544620]

(39). Weber P; Wagner M; Schneckenburger H. Fluorescence imaging of membrane dynamics in living cells. J Biomed Opt 2010, 15 (4), 046017. [PubMed: 20799819]

(40). Monzel C; Fenz SF; Merkel R; Sengupta K. Probing biomembrane dynamics by dual-wavelength reflection interference contrast microscopy. Chemphyschem 2009, 10 (16), 2828–2838. [PubMed: 19821476]

(41). Tuvia S; Levin S; Bitler A; Korenstein R. Mechanical fluctuations of the membrane-skeleton are dependent on f-actin atpase in human erythrocytes. J Cell Biol 1998, 141 (7), 1551–1561. [PubMed: 9647648]

(42). Strey H; Peterson M; Sackmann E. Measurement of erythrocyte membrane elasticity by flicker eigenmode decomposition. Biophys J 1995, 69 (2), 478–488. [PubMed: 8527662]

(43). Steinbrenner DF; Behrends JC. Serotonin-loading increases granule size and prolongs fusion pore formation in two types of rat basophilic leukaemia (rbl) mast cell analogs. Biophys J 2013, 104 (2), 620a–621a.

(44). Cohen R; Corwith K; Holowka D; Baird B. Spatiotemporal resolution of mast cell granule exocytosis reveals correlation with ca^{2+} wave initiation. J Cell Sci 2012, 125 (Pt 12), 2986–2994. [PubMed: 22393234]

(45). Ales E; Tabares L; Poyato JM; Valero V; Lindau M; Alvarez de Toledo G. High calcium concentrations shift the mode of exocytosis to the kiss-and-run mechanism. Nat Cell Biol 1999, 1 (1), 40–44. [PubMed: 10559862]

(46). Ren L; Mellander LJ; Keighron J; Cans AS; Kurczy ME; Svir I; Oleinick A; Amatore C; Ewing AG. The evidence for open and closed exocytosis as the primary release mechanism. Q Rev Biophys 2016, 49, doi:10.1017/S0033583516000081.

(47). Wightman RM; Haynes CL. Synaptic vesicles really do kiss and run. Nat Neurosci 2004, 7 (4), 321–322. [PubMed: 15048116]

(48). Alvarez De Toledo G; Fernandez-Chacon R; Fernandez JM. Release of secretory products during transient vesicle fusion. Nature (London) 1993, 363 (6429), 554–558. [PubMed: 8505984]

(49). Amatore C; Bouret Y; Travis ER; Wightman RM. Interplay between membrane dynamics, diffusion and swelling pressure governs individual vesicular exocytotic events during release of adrenaline by chromaffin cells. Biochimie 2000, 82 (5), 481–496. [PubMed: 10865134]

(50). Amatore C; Oleinick AI; Svir I. Reconstruction of aperture functions during full fusion in vesicular exocytosis of neurotransmitters. Chemphyschem 2010, 11 (1), 159–174. [PubMed: 19937905]

(51). Wu Z; Su M; Tong C; Wu M; Liu J. Membrane shape-mediated wave propagation of cortical protein dynamics. Nat Commun 2018, 9, doi: 10.1038/s41467-017-02469-1.

(52). Veksler A; Gov NS. Calcium-actin waves and oscillations of cellular membranes. Biophys J 2009, 97 (6), 1558–1568. [PubMed: 19751660]

(53). Yang Y; Liu X; Wang H; Yu H; Guan Y; Wang S; Tao N. Imaging action potential in single mammalian neurons by tracking the accompanying sub-nanometer mechanical motion. ACS Nano 2018, 12 (5), 4186–4193. [PubMed: 29570267]

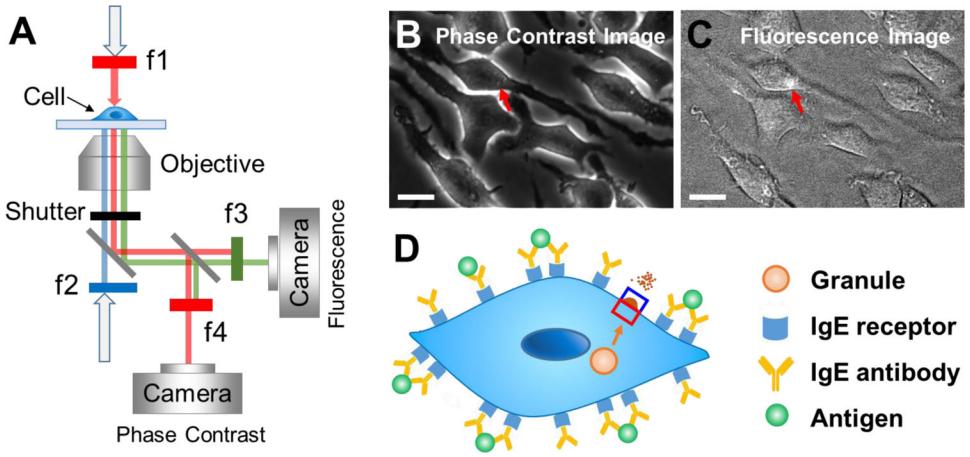

Fig. 1. Detection of vesicle exocytosis by tracking cellular membrane deformation.

(A) Schematic illustration of the setup. A white light source passes through a 600 nm long-pass filter (f1) and illuminates sample cells from the top, and a phase contrast image is recorded by a camera placed behind a second 600 nm long-pass filter (f4). A mercury lamp from the bottom passes a 420–480 nm band filter (f2) and excites FITC-dextran. Fluorescent emission from FITC-dextran is collected with a second camera placed behind a 500–550 nm band filter (f3). A shutter placed at the main optical pathway is used to synchronize phase contrast and fluorescence imaging. (B) Phase contrast image of RBL-2H3 cells, where the red arrow marks the position where a vesicle release occurs. (C) Fluorescence image of RBL-2H3 cells as shown in (B), where the bright spot pointed by the red arrow is due to fluorescence emission from vesicle release. (D) Illustration of vesicle release initiation in RBL-2H3 cells and tracking of the associated cell deformation with a differential optical detection algorithm, where the red and blue rectangles mark the region of interest (ROI). Scale bar: 20 μm.

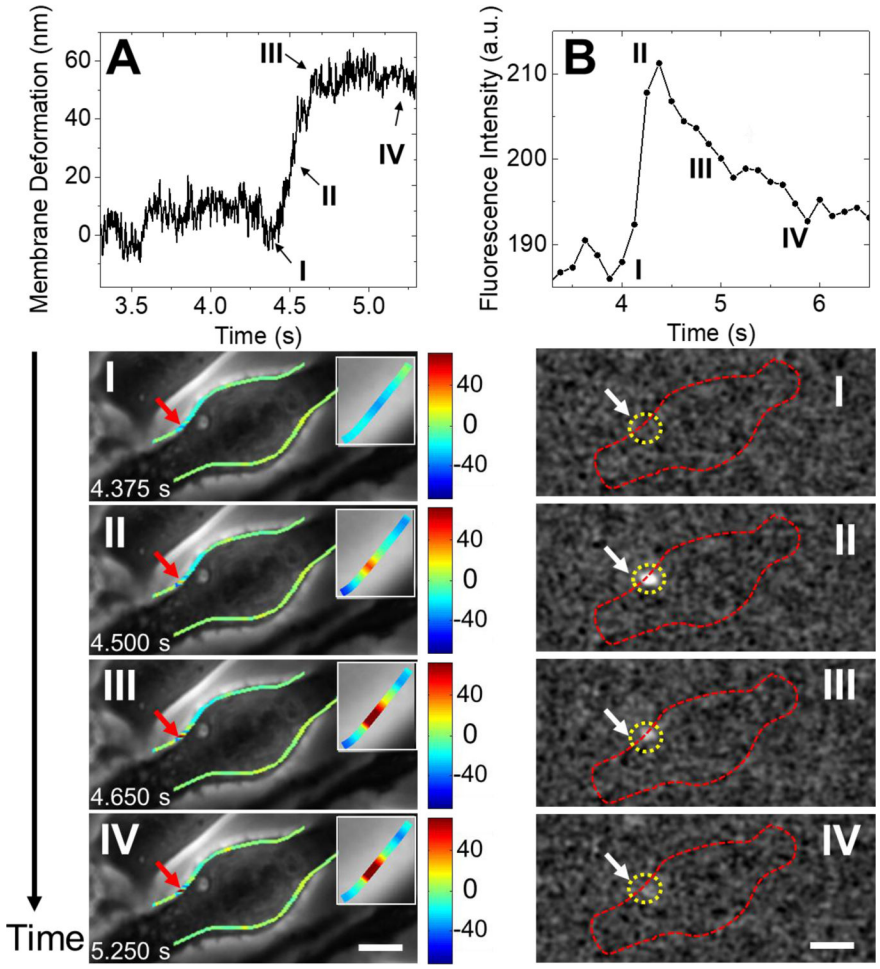

Fig. 2. A representative vesicle release event and the associated membrane responses.

(A) Top: Temporal profile of stepwise deformation at the location of vesicle release. Bottom: Snapshots of phase contrast images at the time points marked by I, II, III and IV along the temporal profile, where the red arrows mark the location of vesicle release, and insets are zoom-in images of the cell deformation location. (B) Top: Temporal profile of fluorescence intensity during the vesicle release event shown in (A). Bottom: Snapshots of the fluorescent images at the time points marked by I, II, III, and IV (first frame subtracted out), where the yellow dashed circles mark the location of vesicle release and the red dashed lines mark the cell edge. Scale bar: 10 μm.

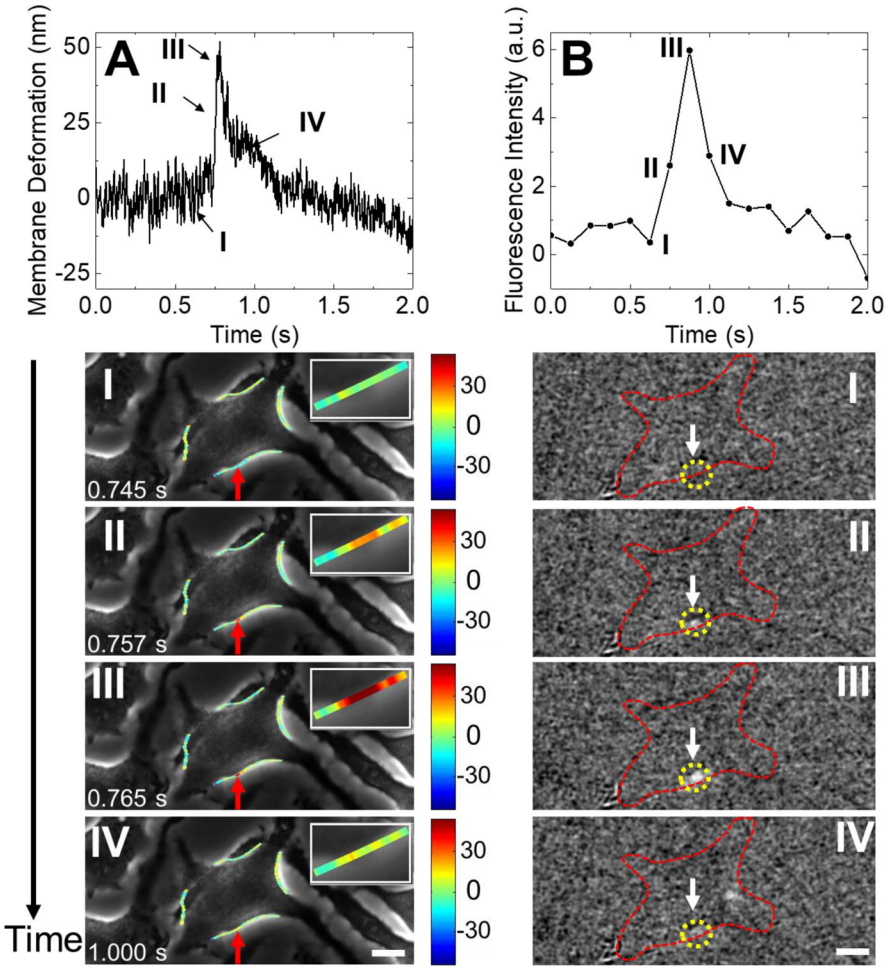

Fig. 3. A vesicle release event and the associated membrane responses.

(A) Top: Temporal profile of pulse-like deformation at the location of vesicle release. Bottom: Snapshots of phase contrast images at the time points marked by I, II, III and IV along the temporal profile, where the insets are zoom-in images of the cell deformation location. (B) Top: Temporal profile of the fluorescence intensity recorded during the vesicle release event shown in (A). Bottom: Snapshots of the fluorescent images at the time points marked by I, II, III, and IV (first frame subtracted out), where the yellow dashed circles mark the location of vesicle release and the red dashed lines mark the cell edge. Scale bar: 10 μm.

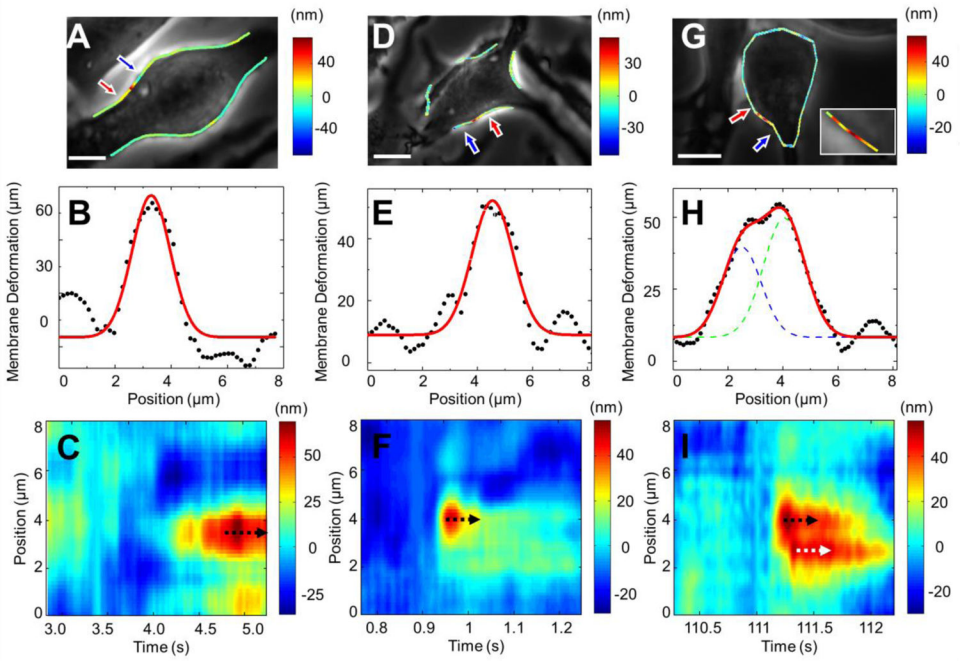

Fig. 4. Spatial distribution and temporal evolution of vesicle-release induced cell deformation.

(A, D and G) Phase contrast images of three cells exhibiting different behaviors, where the colored lines represent the magnitude of cell deformation. The inset in G is the zoom-in image showing two vesicle release events. (B, E and H) Spatial distributions of cell deformation along cell edges marked by the red and blue arrows in the corresponding cells shown in A, D and G, where the black dots are the experimental data and the red lines are Gaussian fitting to the experimental data. (C, F and I) Kymographs of cell deformation for the cells shown in A, D and G, respectively, where the color scale represents the magnitude of the deformation. Scale bar: 10 μm.

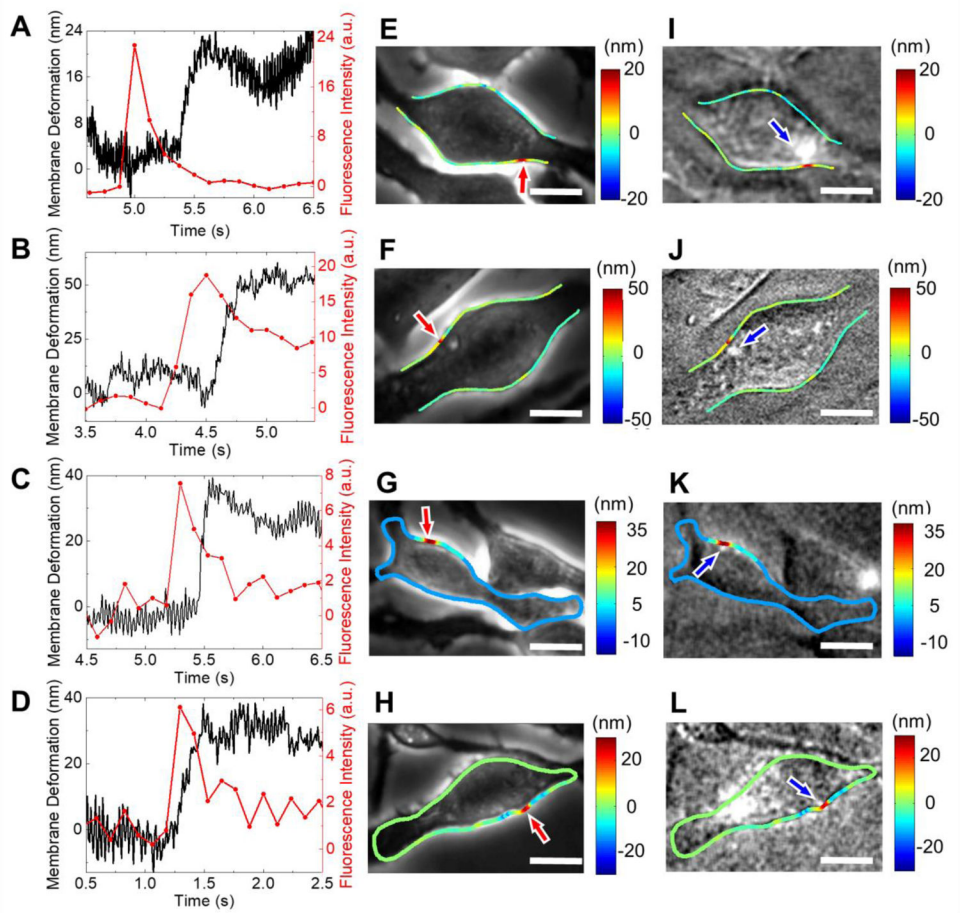

Fig. 5. Propagation of exocytosis-induced cell membrane deformation on cell surfaces.

(A-D) Temporal profiles of cell membrane deformation (black) and corresponding fluorescence signals (red) associated with vesicle release in different RBL-2H3 cells. (E-H) Phase contrast images of the corresponding cells, where the red arrows indicate the locations of the membrane deformation and colored spots represent the magnitudes of the local membrane deformation in nm. (I-L) Fluorescence images of the cells shown in (E-H), where the colored lines represent the local membrane deformation. Scale bar: 10 μm.

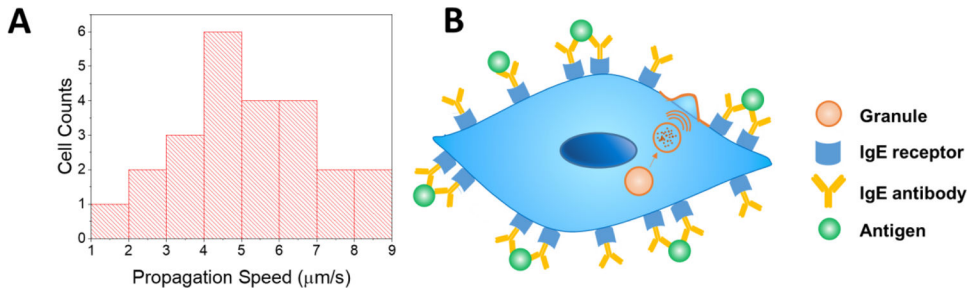

Fig. 6. Propagation speed of vesicle release-induced membrane deformation on cell surface.

(A) Distribution of the propagation speed in different cells. The mean speed is 5.2 μm/s and the standard deviation is 1.8 μm/s (n=24). (B) Schematic illustration of the membrane deformation propagation from the place where the vesicle release occurs to the cell edge.